Digest Journal of Nanomaterials and Biostructures Vol. 19, No. 4, October-December 2024, p. 1361-1369

# Sustainable degradation of AZO dyes using green synthesized lead nanoparticles and solar energy

C. Ramalakshmi[a], S. Shibila[b], R. Mariselvam[c], G. Vijayarani[d,*], V. T. Parameshwari[d], R. Krishnamoorthy[e], M. K. Gatasheh[f]
[a]*DMI - St.Eugene University, Chibombo, Zambia*
[b]*Department of Biotechnology, Meenaakshi Ramasamy Arts and Science College, Thathanur -621804, Ariyalur, Tamil Nadu, India*
[c]*Saraswathi Institute of Lifescience, Alangulam Main Road, Terkkumadathur, Tenkai -627423, Tamil Nadu, India*
[d]*Tamil Institute of Technology, Seeniyapuram, Tenkasi-627423, Tamil Nadu, India*
[e]*Department of Food Science and Nutrition, College of Food and Agriculture Sciences, King Saud University, Riyadh 11451, Kingdom of Saudi Arabia*
[f]*Department of Biochemistry, College of Science, King Saud University, P.O.Box 2455, Riyadh, 11451, Saudi Arabia*

This study explores the green synthesis of lead nanoparticles and their application in degrading the AZO dye Nicoracine under solar irradiation. UV-Visible spectroscopy confirmed nanoparticle formation with a peak at 248 nm, indicating SPR. FTIR revealed functional groups from plant extracts aiding stabilization. XRD analysis showed a crystalline structure, while SEM and AFM indicated irregular shape and rough surface. The nanoparticles exhibited significant catalytic activity, enhancing Nicoracine degradation via solar light, facilitated by ROS generation. Kinetic analysis suggested a pseudo-first-order reaction model. This green synthesis method offers a sustainable solution for wastewater treatment and industrial pollution mitigation.

(Received June 11, 2024; Accepted September 5, 2024)

*Keywords*: Green synthesis, Lead nanoparticles, AZO dye degradation, Solar irradiation, Photocatalysis, Environmental remediation

## 1. Introduction

Nicoracine dye, also known as niacrocine or niacorocine, is a synthetic organic compound belonging to the azo dye class [1]. It is characterized by its vibrant red-orange color and is commonly used as a colorant in various industries, including textiles, cosmetics, and food [2]. Nicoracine dye is derived from the coupling reaction between diazonium salts and naphthols or phenols, resulting in the formation of azo compounds with distinctive chromophoric properties [1]. In the textile industry, nicoracine dye is widely employed for dyeing natural and synthetic fibers, imparting vivid and durable colors to fabrics [3]. Its excellent colorfastness, lightfastness, and washfastness make it a popular choice for producing a wide range of colored textiles, including clothing, upholstery, and home furnishings [4]. Nicoracine dye is prized for its versatility, allowing for the creation of an extensive palette of hues, from vibrant oranges and reds to softer pastel shades [5].

Beyond textiles, nicoracine dye finds applications in cosmetics and personal care products, where it is used to impart color to lipsticks, nail polishes, hair dyes, and skincare formulations [2]. Its vibrant hues and stability make it a favored choice for enhancing the aesthetic appeal of cosmetic products while ensuring long-lasting color intensity [6]. In the food industry, nicoracine dye is approved for use as a color additive in certain food and beverage products, where it imparts a visually appealing red-orange hue [7]. It is commonly used in processed foods, confectionery,

* Corresponding author: vijayarani.g226@gmail.com
https://doi.org/10.15251/DJNB.2024.194.1361

beverages, and dairy products to enhance their appearance and appeal to consumers [7]. Strict regulations govern the use of nicoracine dye in food products to ensure its safety and compliance with food safety standards [8].

Despite its widespread use, concerns have been raised regarding the potential health and environmental impacts of nicoracine dye and other azo dyes [9]. Some azo dyes, including nicoracine, have been associated with allergic reactions and skin sensitization in susceptible individuals [10]. Additionally, the release of azo dyes into the environment through wastewater discharge poses risks to aquatic ecosystems and may contribute to water pollution [1]. Nicoracine dye and other azo dyes have been known to cause skin sensitization and allergic reactions in susceptible individuals [10]. Prolonged or repeated contact with nicoracine-dyed textiles or cosmetics can lead to dermatitis, itching, redness, and other allergic skin reactions [11]. Individuals with existing skin conditions or sensitivities may be particularly susceptible to adverse reactions [12]. Inhalation of nicoracine dye particles or fumes, particularly in occupational settings such as dye manufacturing or textile processing facilities, can irritate the respiratory tract and exacerbate existing respiratory conditions [13]. Workers exposed to airborne nicoracine dye may experience symptoms such as coughing, wheezing, shortness of breath, and chest tightness [13].

While the systemic toxicity of nicoracine dye specifically is not well-documented, certain azo dyes have been associated with adverse health effects when ingested or absorbed into the body [14]. Ingestion of food products containing nicoracine dye as a color additive may raise concerns about potential systemic toxicity, although regulatory authorities generally establish safety thresholds to minimize health risks [15]. Some azo dyes, including certain members of the azo dye class to which nicoracine belongs, have been found to possess genotoxic and carcinogenic properties in laboratory studies [16]. While direct evidence linking nicoracine dye to cancer or genetic damage in humans is limited, regulatory agencies such as the International Agency for Research on Cancer (IARC) classify certain azo dyes as possible or probable human carcinogens based on animal studies and mechanistic evidence [16]. The production, use, and disposal of nicoracine dye and other azo dyes can lead to environmental contamination and ecosystem impacts [17]. Azo dyes may persist in the environment, resist degradation, and bioaccumulate in aquatic organisms, posing risks to wildlife and ecosystems [18]. Additionally, certain azo dyes may undergo reductive cleavage in anaerobic environments, producing aromatic amines that are known carcinogens and environmental pollutants [19].

The degradation of nicoracine dye, like other azo dyes, is an essential aspect to consider due to its potential environmental impact and persistence in the environment [18]. Here are some degradation pathways for nicoracine dye: Biological Degradation, Photodegradation, Chemical Degradation, Sorption and Precipitation [20].

The present study deals with the degradation of nicoracine dye by green synthesized lead nanoparticles under solar degradation method.

## 2. Materials and methods

### 2.1. Plant sample collection and preparation

Collect *Terminalia arjuna* tree bark and wash it thoroughly with distilled water to remove any impurities. Dry the bark in shade to preserve its phytochemical constituents. Grind the dried bark into a fine powder using a mortar and pestle. Prepare an aqueous extract by adding the powdered bark to distilled water and boiling the mixture for a specific duration (30 minutes). Filter the extract using filter paper to remove any solid particles, obtaining a clear solution of Terminalia arjuna bark extract. This extract contains phytochemicals like flavonoids, phenolics, and tannins, which act as reducing and stabilizing agents in the synthesis of PbNPs.

### 2.2. Synthesis of lead nanoparticles

Prepare a Lead Acetate solution (0.1M) by dissolving a Lead precursor such as Lead Acetate [Pb(CH3COO)2], in distilled water. The concentration of the Lead salt solution can vary based on the desired nanoparticle size and concentration. Mix the 90 mL of Lead salt solution with the 10mL *Terminalia arjuna* bark extract in a 90:10 ratio. The bark extract acts as a reducing

agent, converting the Lead Acetate into Lead nanoparticles. Stir the reaction mixture at an optimal temperature 60°C for a specific duration (2 hours) to facilitate the reduction process. Monitor the color change of the reaction mixture from the initial color of the Lead salt solution to reddish-brown, indicating the formation of Lead nanoparticles. Once the reaction is complete, allow the mixture to cool to room temperature and then centrifuge it to separate the synthesized PbNPs from the reaction mixture [21].

### 2.3. Characterization of lead nanoparticles

Characterize the synthesized PbNPs using various analytical techniques such as UV-Vis spectroscopy, which can confirm the formation of nanoparticles based on their characteristic absorption peak in the visible range. Use techniques like scanning electron microscopy (SEM) and AFM to determine the size, morphology, and distribution of the synthesized nanoparticles. Employ techniques like X-ray diffraction (XRD) to analyze the crystalline structure of the PbNPs and confirm their identity.

### 2.4. Removal of AZO dye degradation under solar light irradiation

The solar catalytic degradation of Nicoracine using Lead nanoparticles synthesized from *Terminalia arjuna* tree bark. The catalyst was prepared by mixing 10 ml of the green PbNPs with 100 ml of aqueous Nicoracine (II) chloride solution. Solar light was utilized as the energy source for the degradation process, following the method outlined by Mariselvam et al [22]. To assess the degradation of Nicoracine, UV/visible spectrophotometry was employed, with kinetic measurements conducted at ambient temperature under solar radiation. The concentration of Nicoracine was monitored by measuring the optical density (OD) at various time points within the wavelength range of 200–1000 nm.

## 3. Results and discussion

The UV-Visible spectroscopy analysis of the green synthesized lead nanoparticles displayed a prominent absorption peak at 248 nm (Figure 1). This peak is indicative of the successful formation of lead nanoparticles, as it aligns with the typical absorption characteristics of lead nanoparticles synthesized through green chemistry methods. The absorption peak at 248 nm can be attributed to the surface plasmon resonance (SPR) phenomenon, which is a hallmark of metal nanoparticles. SPR occurs due to the collective oscillation of conduction band electrons at the surface of the nanoparticles when excited by specific wavelengths of light [23]. For lead nanoparticles, the observed SPR peak at 248 nm corroborates previous findings, confirming the presence of nanoscale lead particles with characteristic optical properties.

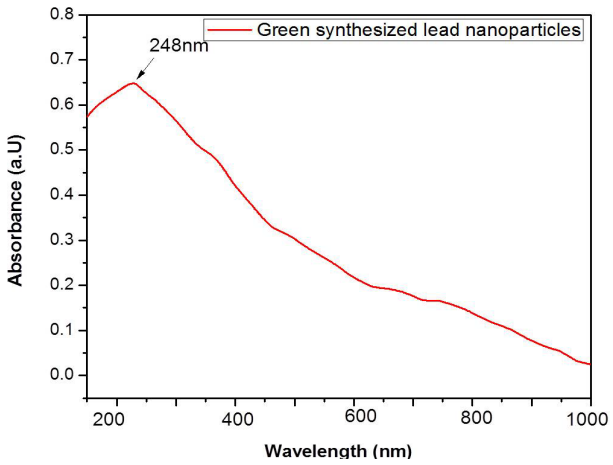


*Fig. 1. UV spectral data of green Synthesized of lead nanoparticles.*

The sharp and intense nature of the absorption peak at 248 nm suggests a narrow size distribution and uniform morphology of the synthesized nanoparticles. A distinct and pronounced peak often indicates that the nanoparticles are monodisperse, meaning they have a consistent size and shape.

The Fourier Transform Infrared (FTIR) spectroscopy analysis of green synthesized lead nanoparticles revealed a range of absorption bands at various wavenumbers, indicating the presence of different functional groups and confirming the successful synthesis of the nanoparticles. The observed absorption bands are as follows (Figure 2). The absorption bands at 347.19 $cm^{-1}$, 362.62 $cm^{-1}$, 393.48 $cm^{-1}$, and 424.34 $cm^{-1}$ can be attributed to metal-oxygen (Pb-O) stretching vibrations. These bands suggest the formation of lead oxide on the surface of the nanoparticles, indicating successful synthesis and stabilization of lead nanoparticles.

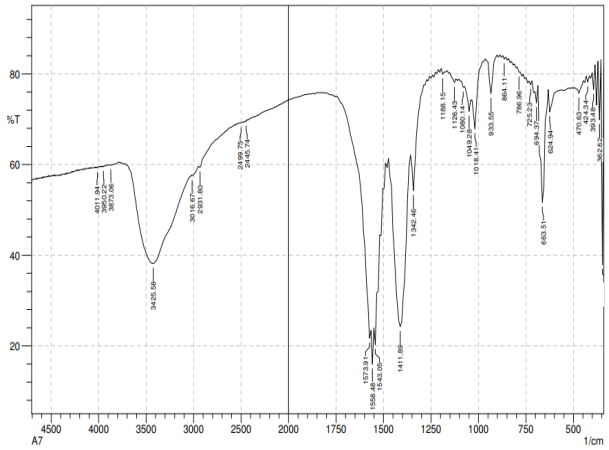


*Fig. 2. FT-IR spectral data of green synthesized of lead nanoparticles.*

The band at 470.63 $cm^{-1}$ also corresponds to Pb-O stretching, reinforcing the presence of lead oxide. The bands at 624.94 $cm^{-1}$, 663.51 $cm^{-1}$, 694.37 $cm^{-1}$, 725.23 $cm^{-1}$, and 786.96 $cm^{-1}$ can be attributed to various bending vibrations of organic compounds, possibly from the phytochemicals in the plant extracts used for the green synthesis. Absorption bands at 864.11 $cm^{-1}$, 933.55 $cm^{-1}$, 1018.41 $cm^{-1}$, 1049.28 $cm^{-1}$, 1080.14 $cm^{-1}$, and 1126.43 $cm^{-1}$ are likely due to C-H bending and C-O stretching vibrations, suggesting the presence of organic moieties. The bands at 1188.15 $cm^{-1}$, 1342.46 $cm^{-1}$, 1411.89 $cm^{-1}$, 1543.05 $cm^{-1}$, 1558.48 $cm^{-1}$, and 1573.91 $cm^{-1}$ can be associated with C=C and C=O stretching vibrations, indicative of carbonyl and alkenyl groups, which are common in plant-derived compounds. Peaks at 2445.74 $cm^{-1}$ and 2499.75 $cm^{-1}$ are related to overtones and combination bands typical of complex organic molecules. The absorption bands at 2931.8 $cm^{-1}$ and 3016.67 $cm^{-1}$ are characteristic of C-H stretching vibrations, which point to the presence of hydrocarbons from the plant extract. Strong absorption bands at 3425.58 $cm^{-1}$, 3873.06 $cm^{-1}$, 3950.22 $cm^{-1}$, and 4011.94 $cm^{-1}$ are indicative of O-H and N-H stretching vibrations, suggesting the presence of hydroxyl and amine groups. These functional groups are crucial for the capping and stabilization of nanoparticles, preventing their aggregation. The metal-oxygen stretching vibrations confirm the formation of lead oxide on the nanoparticle surfaces, which is essential for their stability. The presence of carbonyl, alkenyl, hydroxyl, and amine groups suggests that the bioactive compounds in the plant extract effectively capped the nanoparticles, preventing aggregation and enhancing their stability.

The X-ray diffraction (XRD) analysis of green synthesized lead nanoparticles revealed a single distinct peak at 43.2849° with an intensity of 8.04 counts (Figure 3). This XRD pattern suggests the crystalline nature of the synthesized lead nanoparticles. The single prominent diffraction peak observed at 43.2849° corresponds to a specific crystallographic plane of lead. This peak can be indexed to the (200) plane of face-centered cubic (FCC) lead, indicating that the

nanoparticles exhibit a crystalline structure. The presence of this peak confirms the successful synthesis of lead nanoparticles. The intensity and sharpness of the peak suggest that the nanoparticles have a well-defined crystalline structure. A single, sharp peak indicates that the particles are relatively uniform in size and have a high degree of crystallinity. The relatively low intensity of the peak (8.04 counts) could be attributed to the small quantity of the synthesized material or the presence of amorphous components that do not contribute to the crystalline diffraction pattern. However, the clear presence of the (200) peak is sufficient to confirm the formation of crystalline lead nanoparticles. The XRD analysis has confirmed the successful green synthesis of crystalline lead nanoparticles, characterized by a prominent diffraction peak at 43.2849°. The well-defined crystalline structure of the nanoparticles highlights the effectiveness of using plant extracts in the synthesis process, providing a sustainable and environmentally benign alternative to traditional methods.

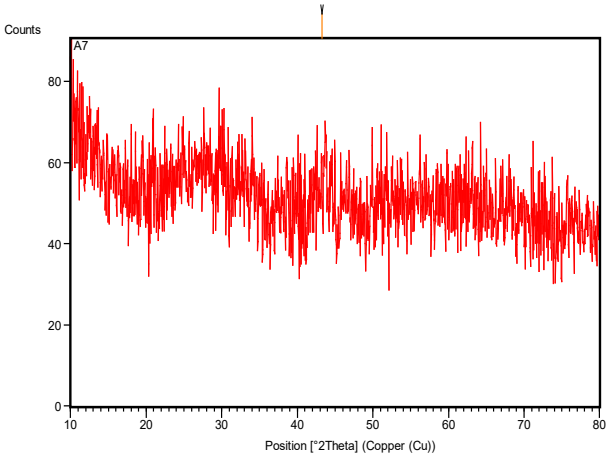


*Fig. 3. XRD spectral data of green Synthesized of lead nanoparticles.*

The estimated crystallite size of the green synthesized lead nanoparticles is approximately 85.54 nm. The surface morphology and shape of the green synthesized nanoparticles were confirmed by SEM and AFM. The synthesized nanoparticles are irregular shape and rough surface (Figure 4 and 5).

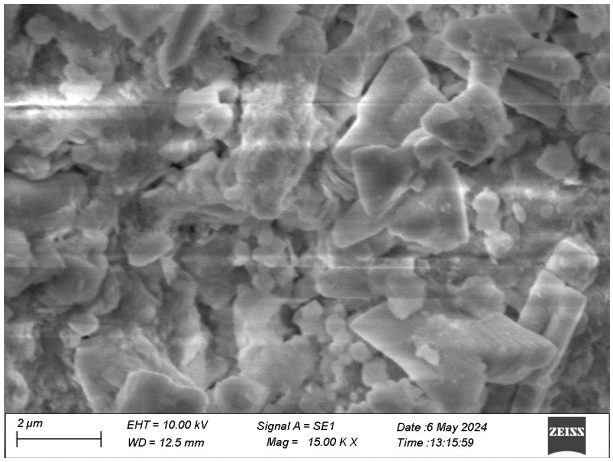


*Fig. 4. SEM images of green Synthesized of lead nanoparticles.*

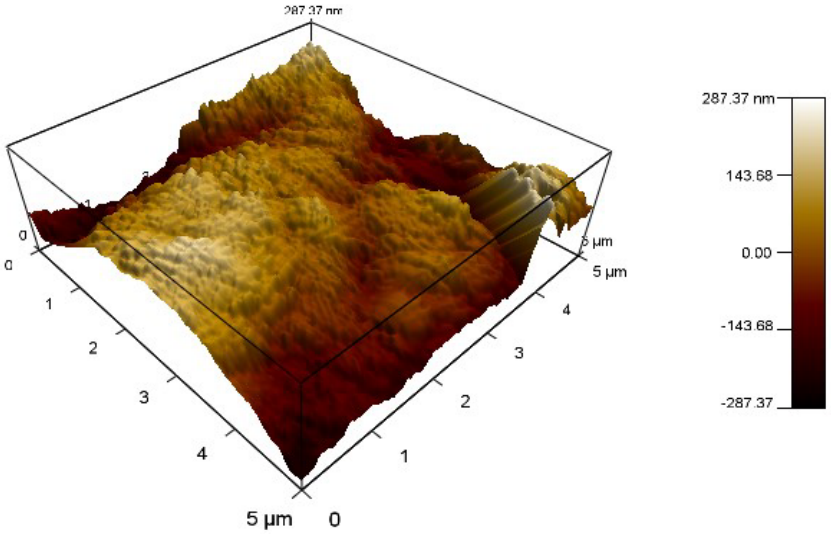


*Fig. 5. AFM of green synthesized of lead nanoparticles.*

The primary outcome the research demonstrates that green synthesized lead nanoparticles significantly enhance the degradation of Nicoracine under solar irradiation (Figure 6). This can be attributed to the unique catalytic properties of lead nanoparticles, which effectively facilitate the breakdown of the dye molecules. The degradation efficiency observed study is likely due to the high surface area and reactive sites provided by the nanoparticles, which interact with the dye molecules under sunlight, accelerating the degradation process. Solar irradiation plays a crucial role in this catalytic process. The photons from sunlight provide the necessary energy to activate the lead nanoparticles, which then generate reactive oxygen species (ROS) such as hydroxyl radicals. These ROS are highly reactive and can break the complex structures of AZO dyes like Nicoracine into simpler, non-toxic molecules. The use of solar energy not only makes the process cost-effective but also environmentally friendly, as it harnesses a renewable energy source. Kinetic analysis likely shows that the degradation of Nicoracine follows a pseudo-first-order reaction model, which is common for photocatalytic processes. The rate constant derived from this model provides insights into the efficiency of the nanoparticles as catalysts. Higher rate constants indicate more efficient catalytic activity, correlating with the effectiveness of the lead nanoparticles in degrading the dye under solar irradiation.

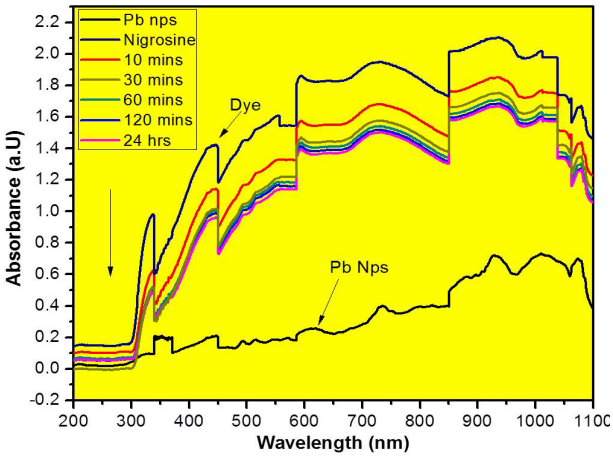


*Fig. 6. Solar catalytic degradation of nicoracine using lead nanoparticles synthesized from T. arjuna tree bark extract.*

Mechanistically, the degradation process involves several steps: absorption of solar photons by the lead nanoparticles, excitation of electrons, and formation of electron-hole pairs. These pairs then participate in redox reactions that generate ROS, which attack the dye molecules. Understanding these steps can help in optimizing the conditions for maximum degradation efficiency, such as adjusting the concentration of nanoparticles, pH of the solution, and intensity of solar exposure.

The successful degradation of Nicoracine using green synthesized lead nanoparticles under solar light suggests a viable method for treating wastewater containing AZO dyes. This approach can be applied to various industrial effluents, potentially reducing the environmental footprint of textile and dyeing industries.

For future research, exploring the recyclability and stability of the lead nanoparticles could provide further insights into their practical application. Additionally, investigating the degradation of a wider range of pollutants using similar green synthesized nanoparticles could establish broader applicability and effectiveness of this method.

The study showcases the potential of combining green chemistry with solar energy to address environmental pollution, particularly in the context of dye degradation. This innovative approach not only contributes to sustainable practices but also offers a promising solution for mitigating the impact of industrial pollutants.

## 4. Conclusion

The study successfully demonstrated the synthesis of lead nanoparticles using green methods and their effective application in the solar catalytic degradation of the AZO dye, Nicoracine. The UV-Visible spectroscopy confirmed the formation of lead nanoparticles, with a prominent absorption peak at 248 nm indicative of surface plasmon resonance. The FTIR spectroscopy revealed various functional groups that stabilized the nanoparticles, while XRD analysis confirmed their crystalline nature with a distinct peak at 43.2849°. SEM and AFM analyses showed that the nanoparticles had an irregular shape and rough surface.

The catalytic degradation experiments under solar irradiation showed that the lead nanoparticles significantly enhanced the breakdown of Nicoracine. This efficiency is attributed to the high surface area and reactive sites of the nanoparticles, which facilitate the generation of reactive oxygen species when activated by sunlight. The kinetic analysis suggested that the degradation followed a pseudo-first-order reaction model, highlighting the efficiency of the nanoparticles as catalysts.

The findings suggest that green synthesized lead nanoparticles are effective for treating wastewater containing AZO dyes, offering a cost-effective and environmentally friendly alternative to traditional methods. Future research should focus on the recyclability and stability of these nanoparticles and explore their application to a broader range of pollutants to establish their versatility and effectiveness.

This study underscores the potential of integrating green chemistry with solar energy to tackle environmental pollution, providing a sustainable and promising solution for reducing the impact of industrial contaminants.

**Acknowledgements**

Authors are thankful to the Researchers Supporting Project **(RSP2024R393),** King Saud University, Riyadh, Saudi Arabia.

## References

[1] S. Benkhaya, S. M'rabet, A. El Harfi, Classifications, properties, recent synthesis and applications of azo dyes. Heliyon, 6(1), e03271(2020); https://doi.org/10.1016/j.heliyon.2020.e03271

[2] P. Brudzyńska, A. Sionkowska, M. Grisel, Materials (Basel, Switzerland), 14(13), 3484(2021); https://doi.org/10.3390/ma14133484

[3] K.L Do, A. Mushtaq, J. Liu, F. Zhao, M. Su, (2024), Fibers and Polymers, 1-12 (2024); https://doi.org/10.1007/s12221-024-00575-8

[4] S.M. Shariful Islam, M. Alam, S. Akter, Fibers and Textiles, 27(1), 1-6 (2020).

[5] B. Leung, Agar Agar: a practice and theory of cultural hybridity in contemporary art (Master's thesis) (2020).

[6] V. Gupta, S. Mohapatra, H. Mishra, U. Farooq, K. Kumar, M.J Ansari, M.F. Aldawsari, A.S Alalaiwe, M.A Mirza, Z. Iqbal, Gels (Basel, Switzerland), 8(3), 173(2022); https://doi.org/10.3390/gels8030173

[7] C.Novais, A.K. Molina, R.M.V Abreu, C. Santo-Buelga, I.C.F.R Ferreira, C. Pereira, L. Barros, Journal of agricultural and food chemistry, 70(9), 2789-2805(2022); https://doi.org/10.1021/acs.jafc.1c07533

[8] R. Varghese, S. Ramamoorthy, Journal fur Verbraucherschutz und Lebensmittelsicherheit = Journal of consumer protection and food safety, 18(2), 107-118(2023); https://doi.org/10.1007/s00003-023-01427-y

[9] K. Ramamurthy, P.S. Priya, R. Murugan, J. Arockiaraj, Environmental science and pollution research international, 10.1007/s11356-024-33444-1(2024).

[10] B. Sadowska, M. Gawinowska, M. Sztormowska, M. Chełmińska, Postepy dermatologii i alergologii, 39(5), 877-879(2022); https://doi.org/10.5114/ada.2021.110263

[11] P.B Murphy, A.R Atwater, M. Mueller, Allergic Contact Dermatitis. In StatPearls. StatPearls Publishing(2023).

[12] L. Chen, J. Zheng, Journal of cosmetic dermatology", 20(7), 2058-2061(2021); https://doi.org/10.1111/jocd.13829

[13] S. Ozkurt, B.A. Kargi, M. Kavas, F. Evyapan, G. Kiter, S. Baser, Journal of environmental research and public health, 9(4)(2012); https://doi.org/10.3390/ijerph9041068

[14] K.T Chung, Journal of environmental science and health. Part C, Environmental carcinogenesis & ecotoxicology reviews, 34(4), 233-261(2016); https://doi.org/10.1080/10590501.2016.1236602

[15] S. Kobylewski, M.F. Jacobson, International journal of occupational and environmental health, 18(3), 220-246(2012); https://doi.org/10.1179/1077352512Z.00000000034

[16] J. Feng, C.E. Cerniglia, H. Chen, Frontiers in bioscience (Elite edition)", 4(2), 568-586(2012); https://doi.org/10.2741/e400

[17] I. Gudelj, J. Hrenović, T.L. Dragičević, F. Delaš, V. Soljan, H. Gudelj, Arhiv za higijenu rada i toksikologiju, 62(1), 91-101(2011); https://doi.org/10.2478/10004-1254-62-2011-2063

[18] S. Zafar, D.A. Bukhari, A. Rehman, Saudi journal of biological sciences, 29(12), 103437(2022); https://doi.org/10.1016/j.sjbs.2022.103437

[19] H. Chen, Current protein & peptide science, 7(2), 101-111(2006); https://doi.org/10.2174/138920306776359786

[20] G. Rajhans, A. Barik, S.K Sen, S. Raut, Biotechnologia, 102(4), 445-455(2021); https://doi.org/10.5114/bta.2021.111109

[21] A. Omidtorshar, M.R. Benam, M. Momennezhad, Z. Sabouri, M. Darroudi, Inorganic Chemistry Communications, 158, 111575(2023); https://doi.org/10.1016/j.inoche.2023.111575

[22] R. Mariselvam, A.J.A. Ranjitsingh, C. Thamaraiselvi, S.I SJ, Journal of King Saud University-Science", 31(4), 1363-1365(2019); https://doi.org/10.1016/j.jksus.2019.07.001

[23] M. Li, S.K Cushing, N. Wu, The Analyst, 140(2), 386-406(2015); https://doi.org/10.1039/C4AN01079E